Geosci. Model Dev., 18, 9791–9803, 2025
https://doi.org/10.5194/gmd-18-9791-2025

Geoscientific Model Development
Open Access
EGU

Comparison of precipitation parameterizations in Regional Climate Model (RegCM5): a case study of the Upper Blue Nile Basin (UBNB)

Eatemad Keshta[1,2], **Doaa Amin**[2], **Ashraf M. ElMoustafa**[1], **and Mohamed A. Gad**[1]

[1]Irrigation and Hydraulics Department, Faculty of Engineering, Ain Shams University, Cairo 11517, Egypt
[2]Water Resources Research Institute (WRRI), National Water Research Center (NWRC), Ministry of Water, Resources and Irrigation (MWRI), Qalyubia 13621, Egypt

Correspondence: Eatemad Keshta (eatemad_hassan@nwrc.gov.eg)

Received: 4 February 2025 – Discussion started: 14 April 2025
Revised: 27 October 2025 – Accepted: 24 November 2025 – Published: 9 December 2025

Abstract. Accurate simulation of precipitation over complex terrains such as the Upper Blue Nile Basin (UBNB) is essential for water resource management and climate impact assessments. The UBNB is characterized by complex terrain and convective precipitation systems that challenge the fine-scale climate simulation processes. This research aims to investigate the best precipitation parameterizations in the Regional Climate Model System (RegCM5) simulating different convective and large-scale schemes over the UBNB domain with 10 km resolution. The RegCM5 is driven by the fifth-generation atmospheric reanalysis (ERA5) for the period of (2000–2009) using the hydrostatic dynamical core. The total precipitation simulations of the different calibration scenarios are assessed to select the optimal RegCM5 configuration over the UBNB. Results show that the model succeeds to capture the dominant spatiotemporal pattern of the precipitation, and the Emanuel scheme coupled with Nogherotto-Tompkins (NoTo) reduces the dominant wet bias in the precipitation simulation. The model highlights challenges in reproducing the UBNB's precipitation variability with a moderate to relatively good correlation of precipitation patterns from 0.46 to 0.77, where deficiency in capturing the large-scale circulations, especially the low-level circulations. The research recommended to focus on dynamics advancement and exploring parameterization schemes that enhance the precipitation representation, such as the Planetary Boundary Layer (PBL) in Future.

1 Introduction

The seasonal rainfall over the Upper Blue Nile Basin (UBNB) is the main determinant of the variability in the entire River Nile basin hydrology, where there is a strong correlation between the fluctuations in both basins' flows (Conway and Hulme, 1993). A more reliable simulation of the UBNB climate, especially rainfall, can help in the water resources management of the riparian countries of the Nile basin. The UBNB is affected by the three Ethiopian climate seasons: Short Rain Season (February–May (FMAM)), Long Rain Season (June–September (JJAS)), and Winter Dry Season (October–January (ONDJ)) (Keshta, 2020). The various atmospheric systems that control the spatiotemporal variations of the UBNB rainfall seasons were comprehensively identified by Camberlin and Philippon (2002), Diro et al. (2011), Fekadu (2015), and Segele and Lamb (2005). The FMAM weather pattern is derived by the interaction between the mid-latitude and tropical weather systems, while during the JJAS, the rainfall onset and distribution follow the Inter-Tropical Convergence Zone (ITCZ) oscillation and the anticyclones intensity of the southern hemisphere. The ONDJ is dominated by the northern hemisphere subtropical anticyclones and dry cool northeasterly monsoon. The JJAS represent the highest proportion of the total UBNB rainfall, with 70 % to exceeding 75 % (Mellander et al., 2013), where the average annual rainfall over the UBNB is around 1200 mm (Amin and Kotb, 2015).

The UBNB climate variability is affected by several global phenomena and mechanisms due to the ocean-atmosphere in-

teraction. Among these mechanisms, the El Niño Southern Oscillation (ENSO) and Indian Ocean Dipole (IOD) are the major drivers of the tropical climate (Coppola et al., 2012; Elsanabary and Gan, 2014; Siam and Eltahir, 2017). ENSO and IOD are phenomena relevant to the teleconnection of the rainfall variability (seasonal to interannual) controlled by the global Sea Surface Temperatures (SSTs). Abtew et al. (2009) found that the dry/wet years of the UBNB were linked to El Niño/La Niña events. El Niño disrupts the moisture transport into the basin, reducing the rainfall, while La Niña enhances it, promoting convective activities and causing heavy rainfall over the UBNB (Conway, 2000). A positive/negative IOD is associated with above/below-average rainfall over the UBNB due to the warm/cool water in the Indian Ocean near Africa (Elsanabary and Gan, 2015). Elsanabary and Gan (2015) also explored the impact of the ENSO and IOD on the UBNB FMAM and JJAS rainy seasons. They found that El Niño increased the FMAM rainfall and decreased the JJAS rainfall, while La Niña showed the opposite effect. However, during FMAM, the UBNB central part is unaffected by ENSO. The IOD has a wet effect on the FMAM and JJAS rainfall. At seasonal timescales, the ITCZ, as the main rain producing system, influences the spatiotemporal variability of rainfall over the UBNB (Tariku and Gan, 2018a; Zaroug et al., 2014). The ITCZ migration is governed by the Earth's tilt, so its effect varies with season due to the UBNB location in the northern hemisphere. During JJAS, the UBNB captures high moisture from the Atlantic Ocean, released by the Ethiopian highlands, due to the developed subtropical high-pressure systems with the blew wind from southwest to northeast together, which followed the ITCZ migration (Camberlin, 2009). Hence, the UBNB southwestern part is exposed to the westerly advective rains for a longer time than the northeast part. In ONDJ, the UBNB is located above the ITCZ, which migrates gradually to the southern hemisphere due to the wind blew from the north to south (Birhan et al., 2019). Therefore, the UBNB couldn't get sufficient precipitation. Moreover, the UBNB has varied topography combining lowlands and high mountains; the Ethiopian Plateau, in which the elevation ranges from 2000 to more than 3500 m a.m.s.l. (Shahin, 1985). This topographic altitude influences the fine-scale spatial distribution of the basin rainfall (Mohamed et al., 2005; Rientjes et al., 2013; Zeleke et al., 2013), since the mountain ranges generate local wind circulation patterns.

The Regional Climate Models (RCMs) can simulate climate over a region of interest at resolutions finer than the Global Circulation Models (GCMs), providing more accurate information. RCMs' performance is usually assessed to investigate the climate characteristics, and study the change of climate as well as land use impacts on the climate variables. A significant challenge in improving RCM performance in the area of interest lies in selecting the most appropriate physical parameterization schemes, developed for a specific climate condition and resolution. Hence, applying identical schemes produces different results not only in different regions but also in different seasons of the same region (Giorgi and Marinucci, 1996). It is demonstrated that the cumulus convection schemes (CCs) have a greater influence on the performance of RCM simulations than other schemes (Li et al., 2023) since CCs control the dynamics and the rainfall regimes variability.

In Africa, especially over Eastern Africa, the Nile basin, and the Sahel region, the versions of the Regional Climate Modelling system (RegCM) and Weather Research and Forecasting (WRF) have been commonly used for different climate applications. Over Eastern Africa, the performance of ten COordinated Regional climate Downscaling Experiment (CORDEX) RCMs forced by European Centre for Medium-Range Weather Forecasts (ECMWF) Interim Re-Analysis (ERA-Interim) was assessed by Endris et al. (2013) in simulating the rainfall. They found an overestimation over the Ethiopian highlands for all RCMs with relatively low spatial correlation; however, the ensembles' mean outperformed the individuals. Tariku and Gan (2018b) applied the WRF over the Nile basin, showing the same rainfall overestimation over the Blue Nile basin in the Ethiopian highlands and demonstrated this result as a predominance of a strong convective regime over the Indian Ocean. Despite this wet bias, they concluded that the Kain-Fritsch CC (Kain, 2004) better simulated the rainfall over the entire basin. Abdelwares et al. (2018) recommended another CC (Betts-Miller-Janjic scheme (BMJ); Janjić, 1994) when developing WRF over the Eastern Nile Basin. Focusing on the UBNB, they found that the combinations that used CCs of Kain-Fritsch and Grell 3D (Grell, 1993) highly overestimated rainfall compared to those that used BMJ, which captured the rainfall annual cycle with a small wet bias during the wet season.

Most studies using the RegCM over eastern Africa also found difficulties in reproducing the rainfall patterns correctly. Segele et al. (2009) used the RegCM3 to simulate eastern Africa, reporting an overestimation of Ethiopia's precipitation when using the Grell and Emanuel (Emanuel, 1991) CCs. Zeleke et al. (2016) evaluated the RegCM4 to simulate the precipitation of rain seasons over the UBNB using the mixed CCs of Grell/Emanuel over land/ocean. Using the initial and boundary conditions of ERA-Interim they found that the precipitation was overestimated over the southwest and central regions and underestimated over the eastern region. Over West Africa, Koné et al. (2018) found that a dry bias dominated the RegCM4 simulation, which was more pronounced using the CC of Tiedtke (1989) and recommended the Emanuel CC when using the RegCM4 with the land surface scheme of CLM4.5 (Community Land Model version 4.5; Oleson et al., 2013).

These selected schemes in previous works are limited due to the coarse model resolution that misses the finer local climate features. The fifth-generation atmospheric reanalysis (ERA5) data provide advancements in the spatiotemporal resolution of $\sim$31 km with 1 h intervals. Compared

with the ERA-Interim, ERA5 improves the vertical coverage, and tropospheric processes and tropical cyclones representation, enhancing the model's ability to simulate the precipitation in the deep tropics (Hoffmann et al., 2019). Therefore, in this study, we aim to evaluate the performance of the latest version of the Regional Climate Model (RegCM5; Giorgi et al., 2023a) over the UBNB using different combinations of convective and large-scale microphysics schemes. The main objective is to identify the most suitable configuration capable of accurately reproducing the observed precipitation characteristics and dominant seasonal variability of the basin. Establishing the optimal RegCM5 configuration over the UBNB will be considered a promising tool for more reliable regional applications, including climate change projection, seasonal forecasting, and the assessment of land use and land cover change impacts.

2 Model Description and Data

The RegCM5 is a freely available and flexible Regional Earth System model. It is the last version of the RCMs series developed at Abdus Salam International Centre for Theoretical Physics (ICTP), which was improved in collaboration with the Institute of Atmospheric Sciences and Climate of the National Research Council (ISAC-CNR) of Italy. A new dynamical core option (the non-hydrostatic core of the weather prediction model MOLOCH) has been added to this new version (Giorgi et al., 2023a). Now there are three options: hydrostatic, non-hydrostatic, and MOLOCH non-hydrostatic to be selected as a dynamical core option for a simulation. The RegCM5 parameterization set comprises various schemes such as the land surface, planetary boundary layer, sea surface flux, cumulus convective, microphysics, and radiation schemes. For the precipitation representation, there are five different cumulus convective schemes and three different microphysics schemes. In addition, mixed convective schemes over land and ocean can be used. More details on the model parameterization schemes can be found in Giorgi et al. (2023b).

The model initial and boundary conditions are driven by atmospheric variables and SST from ERA5 hourly reanalysis data from the ECMWF (Hersbach et al., 2020) with $0.25° \times 0.25°$ horizontal resolution for the period 2000–2009. For evaluation, observed daily rainfall data with a spatial resolution of 20 km × 20 km is obtained for the period of 2001–2009 from the Pre-Processor 7 (PP7). PP7 is a merge between gauge and satellite data blended in the Nile Forecasting System database (NFC, 2009) in the Egyptian Ministry of Water Resources and Irrigation.

Table 1. The domain extent.

Longitude	27° E–53° E
Latitude	5° S–21° N
Nesting Ratio	1 : 3
Resolution	10 km
No. of grid cells	280 × 280
Vertical layers	18 vertical sigma levels
Top pressure	50 hPa

3 Model Setup and Calibration

3.1 Domain

The domain for the RegCM5 simulation over the UBNB is selected to capture both local and large-scale atmospheric processes influencing the precipitation in the region. Figure 1a shows the UBNB domain, while Fig. 1b shows the UBNB topography. The domain has a 10 km resolution and extends from 5° S to 21° N latitude and 27 to 53° E longitude (Fig. 1a), involving the different topographical features and a range of climate zones such as the Ethiopian Highlands, the Western Indian Ocean, the Arabian Peninsula, and the Southern Red Sea. The model utilizes 18 vertical sigma levels and a top at 50 hPa. Table 1 involves the details of the domain extent. The selected domain is large enough to ensure more reliable simulations of the main climate characteristics, among which the moisture transport from the main sources for the region's precipitation dynamics, like the East African Monsoon and the Indian Ocean (Endris et al., 2013).

3.2 Physics Parametrization

The hydrostatic dynamic core (Giorgi et al., 1993) is used for the RegCM5 configuration in the different numerical experiments. To optimize the number of trials due to the high computational cost, the selection of the parameterization schemes representing the precipitation is divided into two parts to be tested over the UBNB, where the second part has resulted from the initial evaluation of the first one, as follows:

1. First, four Cumulus Convective (CC) schemes are tested: Grell (closure of Fritsch-Chappell), Emanuel, Tiedtke, and Kain-Fritsch schemes, to represent the convective precipitation over land. Over the ocean, only the Emanuel scheme is selected as mixed convection with all four CCs over land. The SUB-grid EXplicit (SUBEX) (Pal et al., 2000) is used for large-scale (resolvable, or non-convective) precipitation. The SUBEX is selected as a resolved-scale cloud physics option, which is usually used in the earlier RegCM versions over the UBNB or around the basin, such as Ethiopia, East Africa, and West Africa (Endris et al., 2013; Koné et al., 2018; Nikulin et al., 2012; Segele et al., 2009; Zeleke et al., 2016).

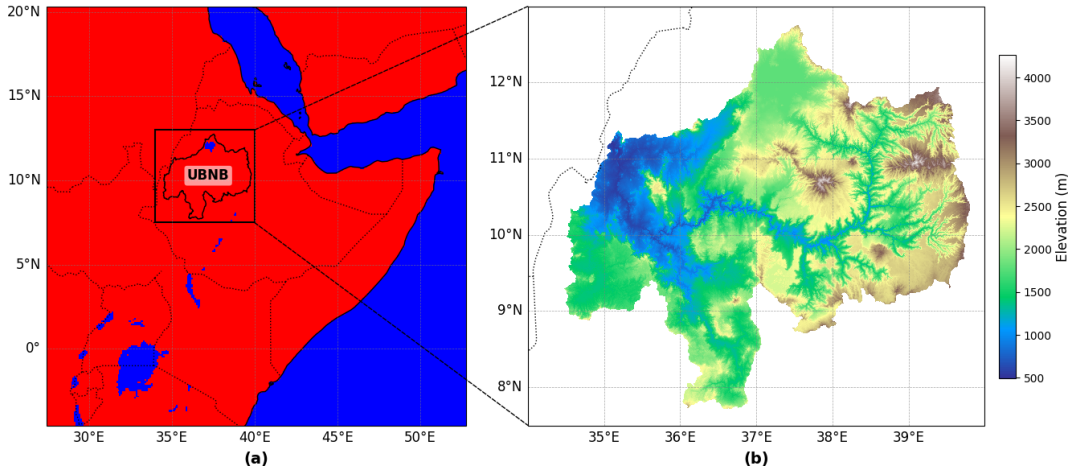

Figure 1. The extent of the UBNB domain. **(a)** Land Mask of the UBNB domain; (red for land and blue for water), and **(b)** UBNB topography; (unit: m).

2. Second, after the initial evaluation of the results, a high overestimation of the precipitation is noticed, especially in the scenario that used the Grell. As a result, the Grell is excluded, and a decision was made to enhance the choice of schemes that can also affect the precipitation simulation. Hence, a new set of simulations was conducted by using Nogherotto-Tompkins (NoTo; Nogherotto et al., 2016) microphysics scheme, which treats the mixed-phase clouds, removing the oversimulation of the upper-level cloud characteristics of the SUBEX scheme. Over East Africa, Gudoshava and Semazzi (2019) revealed that the NoTo generally reduces the overestimation of CCs; however, they recommended the SUBEX with the Grell (Fritsch-Chappell closure). In addition, Kalmár et al. (2021) tested different resolved-scale cloud microphysics schemes over a mountainous region in eastern-central Europe. They found the SUBEX overestimated the high intensity tail of the observed precipitation, while the NoTo reproduced it better, whatever the type of the dynamical core (hydrostatic or non-hydrostatic). Therefore, in this research, the NoTo is added as another option for large-scale precipitation.

The planetary boundary layer (PBL) scheme developed by Holtslag et al. (1990) is used to represent the vertical interaction between the surface (land or ocean) and the atmosphere. In addition, the ocean flux scheme developed by Zeng et al. (1998) is used, and the rapid radiation transfer scheme (RRTM) is used as the radiation scheme. Finally, the CLM4.5 is used for the land surface representation. These schemes are chosen based on recommendations provided in previous studies conducted near the UBNB, as the choice of SUBEX (above). It should be noted that in all convection schemes, the default parameter values are used. Table 2 summarizes the selected parameterization schemes for the seven calibration scenarios.

3.3 Calibration Methodology

Some statistical criteria are used for the performance evaluation of the different physical parametrizations of RegCM5 over the UBNB. Two statistical criteria, relative bias (Bias %), Eq. (1), and Root Mean Squared Error to observation Standard Deviation Ratio (RSR), Eq. (2) (Moriasi et al., 2007), are calculated on a monthly time series basis as an error indication. The monthly mean spatial precipitation over the UBNB is first computed, and then this basin-averaged monthly time series is used to calculate the Bias % and RSR between simulated and observed precipitation. According to Moriasi et al. (2007), model performance is considered satisfactory when RSR ≤ 0.70.

$$\text{Bias}\,\% = \left[\frac{\sum_{t=1}^{n}\left(Y_t^{\text{sim}} - Y_t^{\text{obs}}\right)\cdot 100}{\sum_{t=1}^{n}\left(Y_t^{\text{obs}}\right)}\right], \tag{1}$$

$$\text{RSR} = \left[\frac{\sqrt{\sum_{t=1}^{n}\left(Y_t^{\text{sim}} - Y_t^{\text{obs}}\right)^2}}{\sqrt{\sum_{t=1}^{n}\left(Y_t^{\text{obs}} - \overline{Y^{\text{obs}}}\right)^2}}\right], \tag{2}$$

where n is the number of observations, Y_t^{sim}, Y_t^{obs} are the simulated and observed precipitation at time t, respectively, and $\overline{Y^{\text{obs}}}$ is the mean of the precipitation observations during the calibration period.

To check the annual cycle and spatial distribution, some additional criteria are computed for the three climate seasons FMAM, JJAS, and ONDJ. The correlation coefficient in time

Table 2. Combination of physical parameterization schemes selected for calibration.

Scenario No.	Land CC	Ocean CC	Microphysics	PBL	Ocean Surface Flux	Radiation	Land Surface	Scenario Name
S1	Grell	Emanuel	SUBEX	Holtslag	Zeng	RRTM	CLM4.5	Grell_SUBEX
S2	Emanuel							Emanuel_SUBEX
S3	Tiedtke							Tiedtke_SUBEX
S4	Kain-Fritsch							Kain-Fritsch_SUBEX
S5	Emanuel		NoTo					Emanuel_NoTo
S6	Tiedtke							Tiedtke_NoTo
S7	Kain-Fritsch							Kain-Fritsch_NoTo

is calculated for the three seasons to measure the strength of a linear association between the simulations and observation patterns for each grid point. The correlation coefficient (R^2) is given by Eq. (3).

$$R^2 = \frac{\sum_{t=1}^{n}\left(Y_t^{\text{obs}} - \overline{Y^{\text{obs}}}\right)\left(Y_t^{\text{sim}} - \overline{Y^{\text{sim}}}\right)}{\sigma^{\text{obs}}\,\sigma^{\text{sim}}} \quad , \tag{3}$$

where $\overline{Y^{\text{sim}}}$ is the mean of the simulated, and σ^{obs} and σ^{sim} are the standard deviations of the observed and the simulated precipitation.

Finally, the Brier Score (BS) and Significance Score (SS) (Brier, 1950; Fraedrich and Leslie, 1987), are estimated to assess the probability density function (PDF) for the simulated and observed daily data during the three seasons. A wet day is defined as a day with precipitation greater than 1 mm d^{-1}. This threshold was applied to exclude trace amounts and ensure consistency when evaluating precipitation intensity and frequency. The BS represents the mean square error of the probability, and SS represents the smallest cumulative probability of the observation and simulation distribution in each equal sequence of values. BS and SS are given as follows:

$$\text{BS} = \frac{1}{N}\sum_{i=1}^{N}(P_i^{\text{sim}} - P_i^{\text{obs}})^2, \tag{4}$$

$$\text{SS} = \sum_{i=1}^{N}\text{Minimum}(P_i^{\text{sim}}.\, P_i^{\text{obs}}) \quad , \tag{5}$$

where N is the number of intervals, P_i^{sim} is the probability density value of the simulated precipitation at the interval i, and P_i^{obs} is the probability density value of the observed precipitation at the interval i. The smaller/larger BS/SS indicates the ability of the RegCM5 scheme to simulate the probability density distribution.

4 Results and Discussion

The results are analyzed for the period of 2001–2009 since the year 2000 was considered as a spin-up period. The simulated precipitation is compared to the observed PP7 data.

4.1 Error-based Evaluation

To evaluate the different RegCM5 configurations over the UBNB, Fig. 2 and Table 3 show the evaluation results of the simulated precipitation for the seven numerical experiments. Figure 2a shows the mean monthly precipitation, which represents the mean annual cycle over the UBNB. The annual mean of the PP7 is about 1232 mm. Most of the RegCM5 simulations follow the observed precipitation pattern, but there is a high overestimation, especially for S1, which uses the Grell scheme. It is also noticed that the overestimation is reduced when changing the microphysics scheme from SUBEX to NoTo, indicating that SUBEX overestimates the large-scale precipitation over the UBNB. For NoTo scenarios, both Emanuel and Tiedtke (S5 and S6) are closer to the PP7 than Kain-Fritsch (S7), especially at the onset of the rainy seasons (FMAM and JJAS). The NoTo not only corrects the overestimation but also reduces the difference between the CCs.

To analyze the variation of the three climate seasons (FMAM, JJAS, and ONDJ) over the UBNB, the monthly mean precipitation boxplots are presented in Fig. 2b. It is noticed that NoTo (S5, S6, and S7) succeeded to reduce the precipitation range. In addition, it captures the low rainfall values in the wet season (JJAS). S5 and S6 boxplots are also closer to the PP7 boxplots than the other scenarios. Table 3 reports the computed statistical criteria that investigate the error of the model simulations of the mean areal precipitation over the basin. It is found that the S5 has the lowest and best values of the Bias % and RSR. The RSR is out of the accepted range ($0 \leq \text{RSR} \leq 0.7$); however, as shown in Fig. 3a, all the experiments successfully capture the dominant temporal pattern of rainfall variability. For the considerable wet

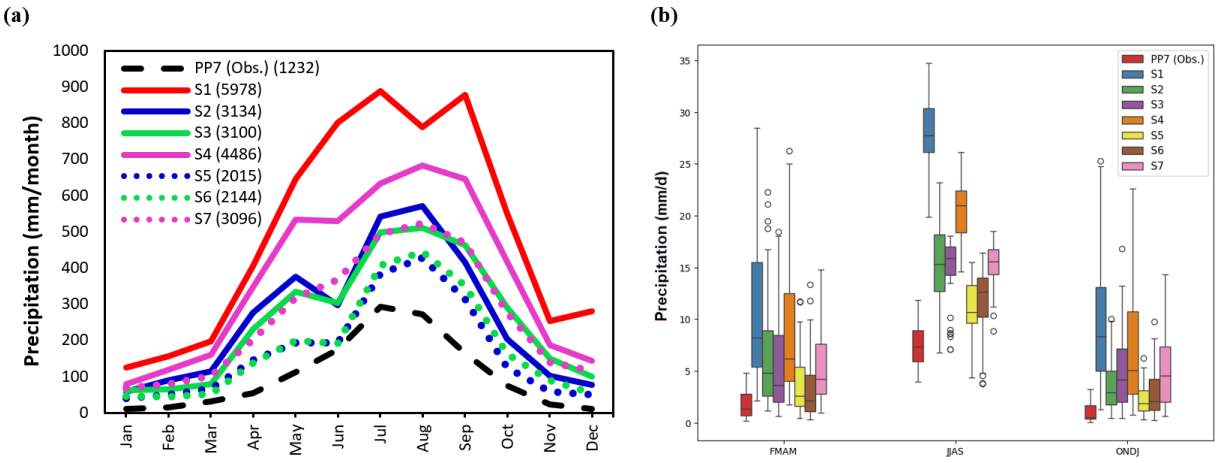

Figure 2. Simulations of precipitation over UBNB; **(a)** the mean monthly, and **(b)** boxplots of the monthly mean during rain and dry seasons.

Table 3. Error-based statistical criteria

Scenario	Bias %	RSR
S1	339	4.60
S2	153	2.10
S3	149	2.00
S4	261	3.25
S5	66	1.00
S6	76	1.20
S7	155	1.90

bias, previous studies have demonstrated that it is important for the RCMs to perform well in capturing the dominant spatiotemporal pattern of the climate variability than the absolute values of the bias. For example, Koné et al. (2018) tested the sensitivity of the RegCM4 to different convective schemes over West Africa. They found that Emanuel succeeded to reduce the dominant dry bias that ranged between 26 % to 43 % over different regions in West Africa. Hence, bias correction is generally required before using the simulated variables for any hydrological impact or application studies (Haerter et al., 2011; Sippel et al., 2016; Teutschbein and Seibert, 2012). For example, Osman et al. (2021) tested the WRF model sensitivity to get its optimum configuration over the Eastern Nile. Their results showed highly underestimated precipitation over the UBNB; therefore, they corrected the simulation using a bias correction method before applying it to the hydrological model.

4.2 Spatiotemporal Evaluation

The performance of the experiments S5, S6, and S7, which use the NoTo microphysics scheme, is evaluated by analyzing the spatial pattern and the intra-annual variability for the three seasons. Figure 3 shows the Bias % with respect to PP7 observation data. The bias distribution indicates that the model tends to overestimate precipitation in the central and southern mountainous regions of the basin, where high rainfall is typically observed. This positive bias is particularly pronounced in the Kain-Fritsch scenario. In contrast, the model also exhibits substantial positive bias over the eastern and southwestern regions, which are semiarid zones that generally receive low precipitation compared to the central and southern parts. The bias distribution shows spatial discontinuities in simulated precipitation, especially in the northeast. These discontinuities are mainly attributed to the strong topographic gradients and land–atmosphere interactions over the northeastern highlands of the basin, where local convective triggering is highly sensitive to terrain-induced uplift and land surface heterogeneity. Emanuel, which has the lowest overestimation, underestimated the precipitation in the western region in JJAS with a negative bias of about 10 %. In the FMAM season, Tiedtke has a slightly lower overestimation than Emanuel.

Figure 4 represents the spatial variation of the correlation coefficient between the monthly mean time series of the simulated precipitation of S5, S6, and S7 and the PP7 observed precipitation during the three seasons. The correlation ranges from 0.46 to 0.77, showing a moderate to relatively good relationship between the simulated and observed precipitation. This indicates that the model captures the temporal variability reasonably well, but the model configurations still need improvement.

All experiments show similar correlation performance with close values across the basin; however, the spatial patterns of correlation provide critical insight into areas where the model exhibits deficiencies. For the FMAM season, weak to moderate correlations dominate most of the basin, and the eastern regions exhibit a lack of strong correlation. In the east of UBNB, short rains during FMAM exhibit a low correlation. In JJAS, the model shows higher correlations in the west, while a negative correlation over the southwestern part.

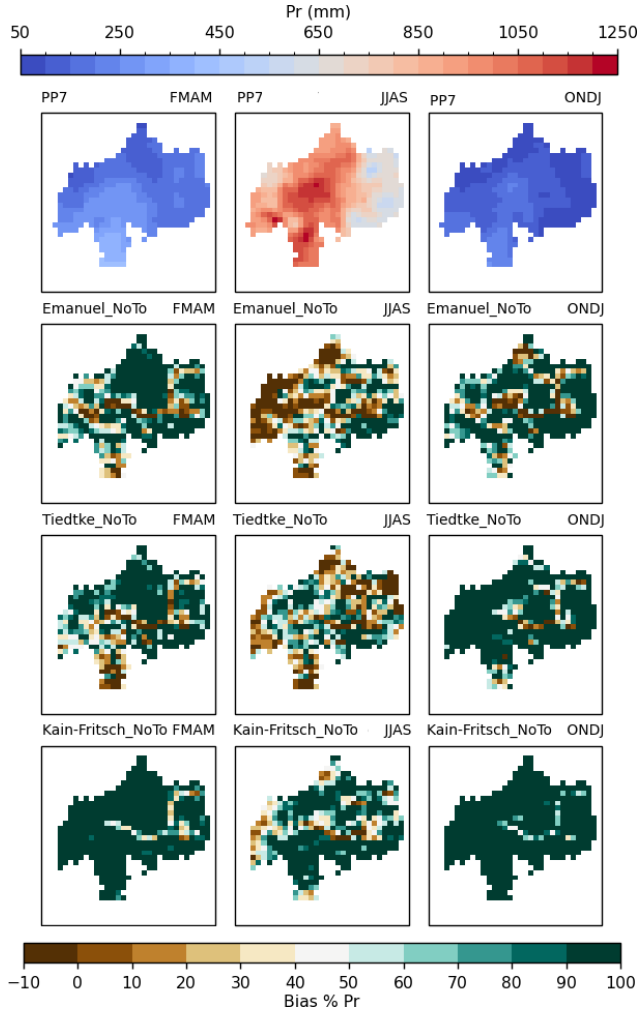

Figure 3. Seasonal mean precipitation relative bias (Bias %) with respect to the PP7 observation data (at the top panel) over the UBNB during the three seasons (FMAM, JJAS, and ONDJ) at (left, middle, and right) columns.

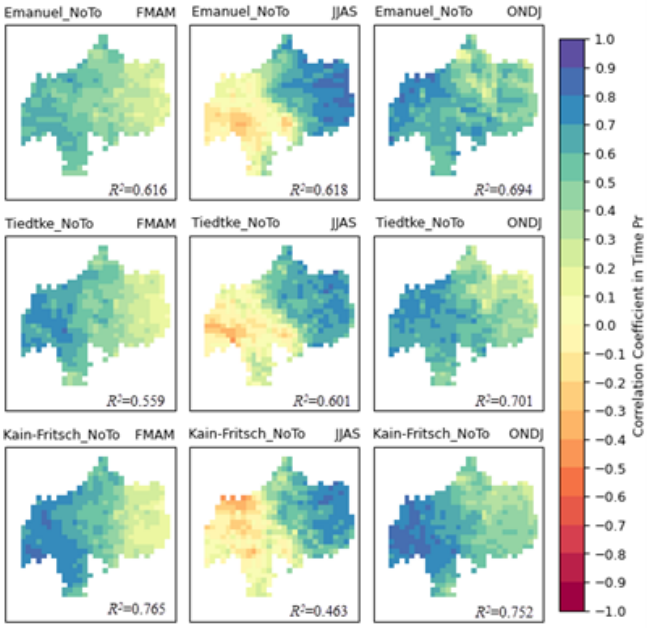

Figure 4. Correlation coefficient with respect to the PP7 observation data over the UBNB during the three seasons (FMAM, JJAS, and ONDJ) at (left, middle, and right) columns.

The PDFs are analyzed to assess the daily precipitation characteristics simulated in the experiments S5, S6, S7 and observed by PP7 during the FMAM, JJAS, and ONDJ (Fig. 5). The simulations couldn't capture the PDF of PP7, especially the low and mid precipitation intensity, which is very clear during the JJAS (Fig. 5b). However, the PDF of Emanuel_NoTo (S5) is closer to the PP7 than the other simulations. Tiedtke_NoTo (S6) slightly better represents the observed distribution of the daily precipitation during the FMAM (Fig. 5a).

The BS and SS scores are reported in Table 4 to evaluate the PDFs. Emanuel_NoTo (S5) has the lowest BS and the highest SS (best results) during JJAS and ONDJ, while for FMAM, the best BS and SS are found when using Tiedtke_NoTo (S6). This demonstrates the visualization interpretation from Fig. 5. The intensity of precipitation events is also influenced by the positioning and dynamics of upper-level jets and troughs (Qi et al., 2023). Therefore, RegCM5 may face challenges in accurately representing these complex interactions due to limitations in parameterizations and resolution. Refining the spatial scale increases the natural variability of the precipitation, challenging the detection of forced signals (Giorgi, 2002). Hence, at such high-resolution simulation, hydrostatic dynamics may struggle to correctly parameterize interactions between local and large-scale circulations. It should also be noted that the observed data may be affected by significant uncertainties. The PP7 is a merge between gauges, collected from data summaries provided by the World Meteorological Organization (WMO), and satellite data. The reported records of rain gauges that cover the UBNB are not error-free, since not all the zero readings occurred, but there is a possibility that rainfall occurred but was not reported (Keshta et al., 2019).

Overall, Emanuel with NoTo succeeded to simulate the UBNB precipitation, especially the JJAS, which represents ∼ 70 % of the total annual precipitation over the UBNB. However, the weak correlation in some parts of the UBNB, eastern/southwestern during FMAM/JJAS, reflects the deficiency of the model to simulate the large-scale circulation associated with the rainfall generation during these seasons. During the FMAM rains over Ethiopia, the large-scale convection in the lower troposphere is fostered by the downward bent of the subtropical westerly jet (SWJ) at upper levels (Zeleke et al., 2016). Similarly, (Fekadu, 2015) highlighted that the interaction of the SWJ with deep troughs in the easterly flow enhances upward motion and moisture

Table 4. Scores of PDFs of the simulated daily precipitation over the UBNB.

Scenario	BS			SS		
	FMAM	JJAS	ONDJ	FMAM	JJAS	ONDJ
Emanuel_NoTo	0.0010	0.0007	0.0008	1.17	1.35	1.57
Tiedtke_NoTo	0.0006	0.0010	0.0009	1.31	1.25	1.50
Kain-Fritsch_NoTo	0.0017	0.0024	0.0017	0.96	0.64	1.26

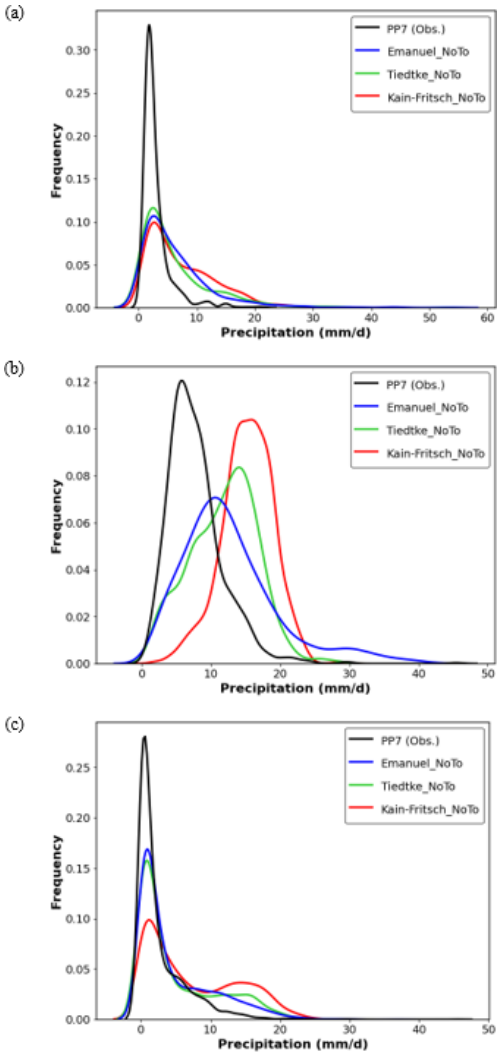

Figure 5. The PDF of the daily precipitation over the UBNB during seasons: **(a)** FMAM, **(b)** JJAS, and **(c)** ONDJ.

convergence, which is critical for rain production during FMAM. For the major long rains during JJAS, the southwestern UBNB is exposed to westerly rains for a longer time than the eastern and northeast parts (Mellander et al., 2013) benefiting from lower tropospheric southwesterlies from the Atlantic (Nicholson, 2017) due to the windward side of the Ethiopian Highlands. These westerly rains are attributed to the large-scale circulation, such as the tropical easterly jet (TEJ) and the Eastern Africa Low-Level Jet (EALLJ). TEJ and EALLJ, with the quasi-permanent high-pressure systems over the South Atlantic and South Indian Ocean, together affect the quality of the JJAS rain season (Camberlin, 2009; Mohamed et al., 2005). The formation and movement of these systems, along with their interactions with local topography and atmospheric conditions, are essential in driving precipitation patterns. For example, large-scale features like the TEJ and shifts in the position of troughs can create instabilities that result in significant rainfall (Yin et al., 2023).

Therefore, the large-scale circulation analysis has been tested for the best performing experiment configuration (Emanuel + NoTo) by comparing the model simulation to the ERA5 reanalysis. Figure 6 shows the model's upper- and lower-level winds compared to the ERA5 reanalysis over the UBNB at 200 and 850 hPa, respectively, during FMAM. The 200 hPa circulation simulated by RegCM5 closely matches ERA5, reproducing the main SWJ structure. However, at 850 hPa, the model overestimates the inflow to the UBNB from the Indian Ocean while underestimating the westerly component originating from the Atlantic Ocean. This imbalance in the simulated low-level circulation likely alters the moisture convergence pattern over the basin. The overintensified easterly-to-southeasterly inflow from the Indian Ocean enhances moisture transport toward the eastern and northern highlands, regions that are typically semi-arid during FMAM. Consequently, this moisture influx can promote excessive convective activity and lead to the positive precipitation bias observed in these regions. Conversely, the underrepresentation of the westerly component reduces the west-to-east advection of moist air masses from the Atlantic and Congo Basin, which normally contribute to the realistic spatial distribution of rainfall. The weakened westerly inflow, therefore, diminishes the dynamic balance between the two moisture sources, resulting in misplaced convergence zones and reduced rainfall correlation with observations in the eastern and northern UBNB.

For the JJAS, Fig. 7 shows the model's upper- and lower-level winds compared to the ERA5 reanalysis over the UBNB at 200 and 850 hPa, respectively. At 200 hPa, the large-scale upper-tropospheric flow is broadly similar between ERA5 and RegCM5, indicating that the model captures the TEJ feature during JJAS. Small differences in jet latitude/intensity are present (the model shows slightly local-

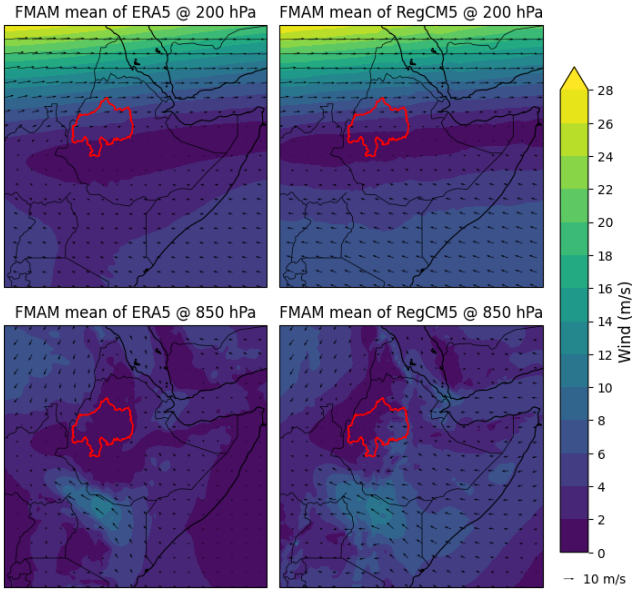

Figure 6. FMAM mean wind ($m\,s^{-1}$; shading) and wind vectors at 200 hPa (upper panels) and 850 hPa (lower panels) from ERA5 (left) and RegCM5 (right) over the UBNB.

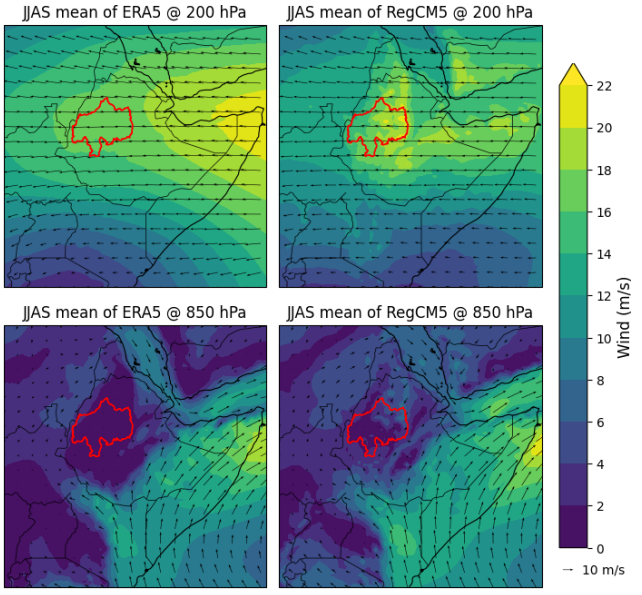

Figure 7. JJAS mean wind ($m\,s^{-1}$; shading) and wind vectors at 200 hPa (upper panels) and 850 hPa (lower panels) from ERA5 (left) and RegCM5 (right) over the UBNB.

ized maxima northeast of the basin), but overall, the upper-level circulation is reproduced reasonably well. At 850 hPa, it is noticed that the model produces an additional northerly/northeastward inflow into the basin that does not exist in ERA5, and at the same time, some of the strong southwesterly flow shown in ERA5 (which brings Atlantic/Congo moisture into the southern and southwestern UBNB) is reduced or displaced. This anomalous northerly contribution in the model reduces the relative importance of the southwesterly moisture supply to the southern and southwestern regions. Because JJAS rainfall in those parts of the basin depends strongly on the low-level southwesterly moisture inflow and convergence on the windward side of the highlands, the model's altered low-level circulation plausibly explains the noticed weak correlation between model and observation.

The good performance of the Emanuel + NoTo configuration likely reflects complementary strengths of the two parameterizations. Emanuel's mass-flux, parcel-based closure is sensitive to environmental humidity and entrainment/detrainment and therefore can better represent convective triggering and organization in orographically influenced regimes (Emanuel, 1991). The NoTo microphysics provides a multiple-phase, prognostic treatment of cloud liquid, ice, rain and snow and yields a more realistic mixed-phase cloud structure and stratiform precipitation (Nogherotto et al., 2016). Together, the Emanuel closure (improved convective moistening and triggering) and NoTo microphysics (improved ice-phase and stratiform processes) change the partitioning between convective and large-scale precipitation and improve the vertical cloud profile, which is especially important in the high-relief, mixed convective/stratiform environment of the UBNB.

However, the model configuration requires enhancement to reduce the bias in the other seasons (FMAM and ONDJ) and generally improve the spatiotemporal pattern over the UBNB. Using the new dynamic core option, MOLOCH non-hydrostatic involved in the RegCM5, may enhance capturing the observed rainfall variability. The non-hydrostatic dynamic core improves the representation of mesoscale convective systems and tropical storms (Giorgi, 2019). Thus, it can resolve fine-scale atmospheric processes circulations in regions with complex terrain and convective precipitation systems such as the UBNB. Silué et al. (2024) found that using MOLOCH non-hydrostatic improves the simulation of precipitation intensity, diurnal cycles, and the representation of mesoscale convective systems compared to the hydrostatic core. They also found that using the PBL scheme of the University of Washington (UW) (Bretherton et al., 2004) instead of its counterpart, Holtslag, showed a better representation of boundary-layer dynamics and vertical mixing. UW employs higher-order turbulence parameterizations and showed outperformance in capturing vertical profiles of temperature, humidity, and wind, leading to improved precipitation simulations during the rainy season (JJAS) over West Africa. Counting for such an update can also improve the precipitation simulation over the UBNB.

5 Conclusions

In this research, we investigated the performance of the RegCM5 (hydrostatic dynamical core), using the advancement of the spatiotemporal resolution of the ERA5, to simulate the spatiotemporal variability of the precipitation over the UBNB for the wet and dry seasons. The model captures the general pattern of the observed rainfall, although it is overestimated compared to the PP7 observation data. The non-convective precipitation is highly overestimated. The NoTo microphysics scheme outperforms the SUBEX in representing the non-convective precipitation and reduces the biases in the simulated total precipitation. Exploring the better performance of NoTo than SUBEX, which has widely been used in earlier studies, especially over East Africa, is considered a novelty of the research. Emanuel CC over land demonstrates a relatively accurate representation of convective precipitation, which dominates rainfall in UBNB, especially during the long rain season (JJAS). During JJAS, the model spatially captures the high rainfall locations in central and southern regions; however, it underestimated the western UBNB with a negative bias of up to 10 %. Due to the high overestimation, the model couldn't capture the low and mid intensities, which is clearly noticed in the daily PDFs.

Comparing the temporal correlation between the simulations and observation data spatially provides critical insight into areas where the model exhibits deficiencies. The model exhibits limited capability in reproducing the spatial rainfall distribution over the eastern (southwestern) parts of the basin during FMAM (JJAS), leading to weak or negative correlations with the observed datasets. The large-scale circulation analysis reveals that these deficiencies are linked to misrepresented low-level wind structures. During FMAM, the RegCM5 simulation overestimates the easterly inflow from the Indian Ocean while underrepresenting the westerly contribution from the Atlantic Ocean, thereby distorting the moisture convergence and increasing the rainfall over the basin. Conversely, in JJAS, the model generates an anomalous northerly component and weakens the southwesterly monsoon flow responsible for transporting moist air from the Atlantic and Congo regions toward the Ethiopian highlands. This deviation in the simulated low-level circulation likely alters the moisture transport pathways and weakens the rainfall–circulation coupling over the UBNB.

In conclusion, the model reasonably succeeded to simulate the dominant spatiotemporal annual pattern of the precipitation over the UBNB using Emanuel with NoTo, since it reproduces the UBNB mean annual close to the PP7 observation data with a wet bias. The success of the model in capturing the spatial variability of the JJAS with a slight dry bias, which represents the highest proportion of the UBNB annual precipitation (~ 70 %), is promising for future enhancement. To enhance the model configuration, we recommend using the new dynamic core option of MOLOCH non-hydrostatic that can play a role in resolving these upper-atmosphere processes, reducing biases in simulating the precipitation. In addition, we recommend to test more physical parameterizations of the RegCM5 that affect the precipitation simulation (e.g., PBL schemes).

Code and data availability. The RegCM5 code is available from the project website: https://github.com/graziano-giuliani/RegCM/tree/5.0.0 (last access: 2 February 2025). The RegCM5 used to produce the results used in this paper is archived at Zenodo (https://doi.org/10.5281/zenodo.7548172, Giorgi et al., 2023a). The model input data is available at http://clima-dods.ictp.it/regcm4 (last access: 2 February 2025). The ERA5 reanalysis data are available at https://doi.org/10.24381/cds.bd0915c6 (Hersbach et al., 2023a) for the initial and boundary conditions, and https://doi.org/10.24381/cds.adbb2d47 (Hersbach et al., 2023b) for the SST data. The observed precipitation data (PP7) used in this research are provided by the Egyptian Ministry of Water Resources and Irrigation (WMRI) and cannot be shared publicly due to data restrictions. The results and codes used to produce the plots for all the simulations presented in this paper are uploaded to Zenodo (Keshta, 2025, https://doi.org/10.5281/zenodo.14864918).

Author contributions. EK was responsible for software development, formal analysis, investigation, data curation, writing the original draft and visualization; EK and DA provided the resources; DA, AME and MAG supervised the research; EK, DA, AME and MAG contributed equally in conceptualization, methodology, validation and writing – review and editing.

Competing interests. The contact author has declared that none of the authors has any competing interests.

Disclaimer. Publisher's note: Copernicus Publications remains neutral with regard to jurisdictional claims made in the text, published maps, institutional affiliations, or any other geographical representation in this paper. While Copernicus Publications makes every effort to include appropriate place names, the final responsibility lies with the authors. Views expressed in the text are those of the authors and do not necessarily reflect the views of the publisher.

Acknowledgements. The authors would like to express their sincere thanks to the Nile Forecast Center, Ministry of Water Resources and Irrigation (MWRI), Egypt, for providing the rainfall data of the NFS. The authors also gratefully acknowledge the Science, Technology & Innovation Funding Authority (STDF) for supporting this paper work under the 2nd Post Graduate Support Grant (PGSGII).

Financial support. This research is supported through a project entitled "Projection of Stored Water Upstream Dams on Microclimate" (no. 48620), which is funded by STDF in Egypt.

Review statement. This paper was edited by Charles Onyutha and reviewed by two anonymous referees.

References

Abdelwares, M., Haggag, M., Wagdy, A., and Lelieveld, J.: Customized framework of the WRF model for regional climate simulation over the Eastern Nile basin, Theor. Appl. Climatol., 134, 1135–1151, 2018.

Abtew, W., Melesse, A. M., and Dessalegne, T.: El Niño Southern Oscillation link to the Blue Nile River Basin hydrology, Hydrol. Process., 23, 3653–3660, 2009.

Amin, D. and Kotb, A.: Assessment of the Skill of Seasonal Meteorological Forecasts in the Eastern Nile, Nile Water Science & Engineering Journal, 8, 31–40, 2015.

Birhan, M. W., Raju, U. J. P., and Kenea, S. T.: Estimating the role of upper Blue Nile basin moisture budget and recycling ratio in spatiotemporal precipitation distributions, J. Atmos. Sol. Terr. Phys., 193, 105064, https://doi.org/10.1016/j.jastp.2019.105064, 2019.

Bretherton, C. S., McCaa, J. R., and Grenier, H.: A New Parameterization for Shallow Cumulus Convection and Its Application to Marine Subtropical Cloud-Topped Boundary Layers. Part I: Description and 1D Results, Mon. Weather Rev., 132, 864–882, 2004.

Brier, G. W.: Verification of Forecasts Expressed in terms of Probability, Mon. Weather Rev., 78, 1–3, 1950.

Camberlin, P.: Nile Basin Climates, in: The Nile: Origin, Environments, Limnology and Human Use, edited by: Dumont, H. J., Monographiae Biologicae, Springer, 307–333, ISBN 978-1-4020-9725-6, 2009.

Camberlin, P. and Philippon, N.: The East African March–May Rainy Season: Associated Atmospheric Dynamics and Predictability over the 1968–97 Period, J. Clim., 15, 1002–1019, 2002.

Conway, D.: The Climate and Hydrology of the Upper Blue Nile River, Geogr. J., 166, 49–62, 2000.

Conway, D. and Hulme, M.: Recent fluctuations in precipitation and runoff over the Nile sub-basins and their impact on main Nile discharge, Clim. Change, 25, 127–151, 1993.

Coppola, E., Giorgi, F., Mariotti, L., and Bi, X.: RegT-Band: a tropical band version of RegCM4, Clim. Res., 52, 115–133, 2012.

Diro, G. T., Grimes, D. I. F., and Black, E.: Large Scale Features Affecting Ethiopian Rainfall, in: African Climate and Climate Change: Physical, Social and Political Perspectives, edited by: Williams, C. J. R. and Kniveton, D. R., Springer Netherlands, Dordrecht, 13–50, https://doi.org/10.1007/978-90-481-3842-5_2, 2011.

Elsanabary, M. H. and Gan, T. Y.: Wavelet Analysis of Seasonal Rainfall Variability of the Upper Blue Nile Basin, Its Teleconnection to Global Sea Surface Temperature, and Its Forecasting by an Artificial Neural Network, Mon. Weather Rev., 142, 1771–1791, 2014.

Elsanabary, M. H. and Gan, T. Y.: Evaluation of climate anomalies impacts on the Upper Blue Nile Basin in Ethiopia using a distributed and a lumped hydrologic model, J Hydrol (Amst), 530, 225–240, 2015.

Emanuel, K. A.: A Scheme for Representing Cumulus Convection in Large-Scale Models, Journal of Atmospheric Sciences, 48, 2313–2329, 1991.

Endris, H. S., Omondi, P., Jain, S., Lennard, C., Hewitson, B., Chang'a, L., Awange, J. L., Dosio, A., Ketiem, P., Nikulin, G., Panitz, H.-J., Büchner, M., Stordal, F., and Tazalika, L.: Assessment of the Performance of CORDEX Regional Climate Models in Simulating East African Rainfall, J. Clim., 26, 8453–8475, 2013.

Fekadu, K.: Ethiopian Seasonal Rainfall Variability and Prediction Using Canonical Correlation Analysis (CCA), Earth Sciences, 4, 112–119, 2015.

Fraedrich, K. and Leslie, L. M.: Evaluation of Techniques for the Operational, Single Station, Short-Term Forecasting of Rainfall at a Midlatitude Station (Melbourne), Mon. Weather Rev., 115, 1645–1654, 1987.

Giorgi, F.: Dependence of the surface climate interannual variability on spatial scale, Geophys. Res. Lett., 29, 14–16, 2002.

Giorgi, F.: Thirty Years of Regional Climate Modeling: Where Are We and Where Are We Going next?, Journal of Geophysical Research: Atmospheres, 124, 5696–5723, 2019.

Giorgi, F. and Marinucci, M. R.: A Investigation of the Sensitivity of Simulated Precipitation to Model Resolution and Its Implications for Climate Studies, Mon. Weather Rev., 124, 148–166, 1996.

Giorgi, F., Marinucci, M. R., and Bates, G. T.: Development of a second generation regional climate model (RegCM2). Part I: Boundary layer and radiative transfer processes, Mon. Weather Rev., 121, 2794–2813, 1993.

Giorgi, F., Coppola, E., Giuliani, G., Ciarlo, J., Pichelli, E., Nogherotto, R., Raffaele, F., Malguzzi, P., Davolio, S., Stocchi, P., and Drofa, O.: RegCM-NH V5 code, Zenodo [code], https://doi.org/10.5281/zenodo.7548172, January 2023a.

Giorgi, F., Coppola, E., Giuliani, G., Ciarlo', J. M., Pichelli, E., Nogherotto, R., Raffaele, F., Malguzzi, P., Davolio, S., Stocchi, P., and Drofa, O.: The Fifth Generation Regional Climate Modeling System, RegCM5: Description and Illustrative Examples at Parameterized Convection and Convection-Permitting Resolutions, Journal of Geophysical Research: Atmospheres, 128, e2022JD038199, https://doi.org/10.1029/2022JD038199, 2023b.

Grell, G. A.: Prognostic Evaluation of Assumptions Used by Cumulus Parameterizations, Mon. Weather Rev., 121, 764–787, 1993.

Gudoshava, M. and Semazzi, F. H. M.: Customization and Validation of a Regional Climate Model Using Satellite Data Over East Africa, Atmosphere (Basel), 10, https://doi.org/10.3390/atmos10060317, 2019.

Haerter, J. O., Hagemann, S., Moseley, C., and Piani, C.: Climate model bias correction and the role of timescales, Hydrol. Earth Syst. Sci., 15, 1065–1079, https://doi.org/10.5194/hess-15-1065-2011, 2011.

Hersbach, H., Bell, B., Berrisford, P., Hirahara, S., Horányi, A., Muñoz-Sabater, J., Nicolas, J., Peubey, C., Radu, R., Schepers, D., Simmons, A., Soci, C., Abdalla, S., Abellan, X., Balsamo, G., Bechtold, P., Biavati, G., Bidlot, J., Bonavita, M., De Chiara, G., Dahlgren, P., Dee, D., Diamantakis, M., Dragani, R., Flemming, J., Forbes, R., Fuentes, M., Geer, A., Haimberger, L., Healy, S., Hogan, R. J., Hólm, E., Janisková, M., Keeley, S., Laloyaux, P., Lopez, P., Lupu, C., Radnoti, G., de Rosnay, P., Rozum, I., Vamborg, F., Villaume, S., and Thépaut, J.-N.: The ERA5 global re-

analysis, Quarterly Journal of the Royal Meteorological Society, 146, 1999–2049, 2020.

Hersbach, H., Bell, B., Berrisford, P., Biavati, G., Horányi, A., Muñoz Sabater, J., Nicolas, J., Peubey, C., Radu, R., Rozum, I., Schepers, D., Simmons, A., Soci, C., Dee, D., and Thépaut, J.-N.: ERA5 hourly data on pressure levels from 1940 to present, Copernicus Climate Change Service (C3S) Climate Data Store (CDS) [data set], https://doi.org/10.24381/cds.bd0915c6, 2023a.

Hersbach, H., Bell, B., Berrisford, P., Biavati, G., Horányi, A., Muñoz Sabater, J., Nicolas, J., Peubey, C., Radu, R., Rozum, I., Schepers, D., Simmons, A., Soci, C., Dee, D., and Thépaut, J.-N.: ERA5 hourly data on single levels from 1940 to present, Copernicus Climate Change Service (C3S) Climate Data Store (CDS) [data set], https://doi.org/10.24381/cds.adbb2d47, 2023b.

Hoffmann, L., Günther, G., Li, D., Stein, O., Wu, X., Griessbach, S., Heng, Y., Konopka, P., Müller, R., Vogel, B., and Wright, J. S.: From ERA-Interim to ERA5: the considerable impact of ECMWF's next-generation reanalysis on Lagrangian transport simulations, Atmos. Chem. Phys., 19, 3097–3124, https://doi.org/10.5194/acp-19-3097-2019, 2019.

Holtslag, A. A. M., Bruijn, E. I. F. De, and Pan, H.-L.: A High Resolution Air Mass Transformation Model for Short-Range Weather Forecasting, Mon. Weather Rev., 118, 1561–1575, 1990.

Janjić, Z. I.: The Step-Mountain Eta Coordinate Model: Further Developments of the Convection, Viscous Sublayer, and Turbulence Closure Schemes, Mon. Weather Rev., 122, 927–945, 1994.

Kain, J. S.: The Kain–Fritsch Convective Parameterization: An Update, Journal of Applied Meteorology, 43, 170–181, 2004.

Kalmár, T., Pieczka, I., and Pongrácz, R.: A sensitivity analysis of the different setups of the RegCM4.5 model for the Carpathian region, International Journal of Climatology, 41, E1180–E1201, 2021.

Keshta, E.: A Multi-Component Model for Long-Term River Flow Forecasting, M.Sc. Thesis, Ain Shams University, Cairo, Egypt, https://doi.org/10.13140/RG.2.2.29798.86089, 2020.

Keshta, E.: Codes and data for the RegCM5 precipitation simulations over the Upper Blue Nile Basin (UBNB), Zenodo, https://doi.org/10.5281/zenodo.14864919, February 2025.

Keshta, E., Gad, M. A., and Amin, D.: A Long–Term Response-Based Rainfall-Runoff Hydrologic Model: Case Study of The Upper Blue Nile, Hydrology, 6, 22, https://doi.org/10.3390/hydrology6030069, 2019.

Koné, B., Diedhiou, A., Touré, N. E., Sylla, M. B., Giorgi, F., Anquetin, S., Bamba, A., Diawara, A., and Kobea, A. T.: Sensitivity study of the regional climate model RegCM4 to different convective schemes over West Africa, Earth Syst. Dynam., 9, 1261–1278, https://doi.org/10.5194/esd-9-1261-2018, 2018.

Li, B., Huang, Y., Du, L., and Wang, D.: Sensitivity experiments of RegCM4 using different cumulus and land surface schemes over the upper reaches of the Yangtze river, Front Earth Sci (Lausanne), 10, https://doi.org/10.3389/feart.2022.1092368, 2023.

Mellander, P.-E., Gebrehiwot, S. G., Gärdenäs, A. I., Bewket, W., and Bishop, K.: Summer rains and dry seasons in the upper Blue Nile Basin: the predictability of half a century of past and future spatiotemporal patterns, PLoS One, 8, e68461, https://doi.org/10.1371/journal.pone.0068461, 2013.

Mohamed, Y. A., van den Hurk, B. J. J. M., Savenije, H. H. G., and Bastiaanssen, W. G. M.: Hydroclimatology of the Nile: results from a regional climate model, Hydrol. Earth Syst. Sci., 9, 263–278, https://doi.org/10.5194/hess-9-263-2005, 2005.

Moriasi, D. N., Arnold, J. G., Liew, M. W. Van, Bingner, R. L., Harmel, R. D., and Veith, T. L.: Model Evaluation Guidlines for Systematic Quantification of Accuracy in Watershed Simulations, Trans ASABE, 50, 885–900, 2007.

NFC: Nile Forecasting System (NFS), Version 6.0. Manual, Nile Forecast Center (NFC), internal report, Ministry of Water Rsources and Irrigation (MWRI), Giza, Egypt, 2009.

Nicholson, S. E.: Climate and climatic variability of rainfall over eastern Africa, Reviews of Geophysics, 55, 590–635, 2017.

Nikulin, G., Jones, C., Giorgi, F., Asrar, G., Büchner, M., Cerezo-Mota, R., Christensen, O. B., Déqué, M., Fernandez, J., Hänsler, A., van Meijgaard, E., Samuelsson, P., Sylla, M. B., and Sushama, L.: Precipitation Climatology in an Ensemble of CORDEX-Africa Regional Climate Simulations, J. Clim., 25, 6057–6078, 2012.

Nogherotto, R., Tompkins, A. M., Giuliani, G., Coppola, E., and Giorgi, F.: Numerical framework and performance of the new multiple-phase cloud microphysics scheme in RegCM4.5: precipitation, cloud microphysics, and cloud radiative effects, Geosci. Model Dev., 9, 2533–2547, https://doi.org/10.5194/gmd-9-2533-2016, 2016.

Oleson, K., Lawrence, D., Bonan, G., Drewniak, B., Huang, M., Koven, C., Levis, S., Li, F., Riley, W., Subin, Z., Swenson, S., Thornton, P., Bozbiyik, A., Rosie, F., Heald, C., Kluzek, E., Lamarque, J.-F., Lawrence, P., Leung, L., and Yang, Z.-L.: Technical description of version 4.5 of the Community Land Model (CLM), https://doi.org/10.5065/D6RR1W7M, 2013.

Osman, M., Zittis, G., Haggag, M., Abdeldayem, A. W., and Lelieveld, J.: Optimizing Regional Climate Model Output for Hydro-Climate Applications in the Eastern Nile Basin, Earth Systems and Environment, 5, 185–200, https://doi.org/10.1007/S41748-021-00222-9, 2021.

Pal, J. S., Small, E. E., and Eltahir, E. A. B.: Simulation of regional-scale water and energy budgets: Representation of subgrid cloud and precipitation processes within RegCM, Journal of Geophysical Research: Atmospheres, 105, 29579–29594, 2000.

Qi, H., Lin, C., Peng, T., Zhi, X., Cui, C., Chen, W., Yin, Z., Shen, T., and Xiang, Y.: Diurnal Characteristics of Heavy Precipitation Events under Different Synoptic Circulation Patterns in the Middle and Lower Reaches of the Yangtze River in Summer, Atmosphere (Basel), 14, https://doi.org/10.3390/atmos14081320, 2023.

Rientjes, T., Haile, A. T., and Fenta, A. A.: Diurnal rainfall variability over the Upper Blue Nile Basin: A remote sensing based approach, International Journal of Applied Earth Observation and Geoinformation, 21, 311–325, 2013.

Segele, Z. T. and Lamb, P. J.: Characterization and variability of Kiremt rainy season over Ethiopia, Meteorology and Atmospheric Physics, 89, 153–180, 2005.

Segele, Z. T., Leslie, L. M., and Lamb, P. J.: Evaluation and adaptation of a regional climate model for the Horn of Africa: rainfall climatology and interannual variability, International Journal of Climatology, 29, 47–65, 2009.

Shahin, M.: Ch2. Physiography of the Nile Basin, in: Hydrology of the Nile, Elsevier Netherlands, Amsterdam, 15–57, ISBN 9780080887562, 1985.

Siam, M. S. and Eltahir, E. A. B.: Climate change enhances interannual variability of the Nile river flow, Nat. Clim. Chang., 7, 350–354, 2017.

Silué, F., Diawara, A., Koné, B., Diedhiou, A., Kouassi, A. A., Kouassi, B. K., Yoroba, F., Bamba, A., Kouadio, K., Tiémoko, D. T., Yapo, A. L. M., Koné, D. I., and Famien, A. M. L.: Assessment of the Sensitivity of the Mean Climate Simulation over West Africa to Planetary Boundary Layer Parameterization Using RegCM5 Regional Climate Model, Atmosphere (Basel), 15, https://doi.org/10.3390/atmos15030332, 2024.

Sippel, S., Otto, F. E. L., Forkel, M., Allen, M. R., Guillod, B. P., Heimann, M., Reichstein, M., Seneviratne, S. I., Thonicke, K., and Mahecha, M. D.: A novel bias correction methodology for climate impact simulations, Earth Syst. Dynam., 7, 71–88, https://doi.org/10.5194/esd-7-71-2016, 2016.

Tariku, T. B. and Gan, T. Y.: Regional climate change impact on extreme precipitation and temperature of the Nile river basin, Clim. Dyn., 51, 3487–3506, 2018a.

Tariku, T. B. and Gan, T. Y.: Sensitivity of the weather research and forecasting model to parameterization schemes for regional climate of Nile River Basin, Clim. Dyn., 50, 4231–4247, 2018b.

Teutschbein, C. and Seibert, J.: Bias correction of regional climate model simulations for hydrological climate-change impact studies: Review and evaluation of different methods, J. Hydrol. (Amst), 456–457, 12–29, https://doi.org/10.1016/J.JHYDROL.2012.05.052, 2012.

Tiedtke, M.: A Comprehensive Mass Flux Scheme for Cumulus Parameterization in Large-Scale Models, Mon. Weather Rev., 117, 1779–1800, 1989.

Yin, J., Yuan, J., Peng, J., Cao, X., Duan, W., Nan, Y., Mao, M., and Feng, T.: Role of the subtropical westerly jet wave train in the eastward-moving heavy rainfall event over southern China in winter: A case study, Front. Earth Sci. (Lausanne), 11, https://doi.org/10.3389/feart.2023.1107674, 2023.

Zaroug, M. A. H., Eltahir, E. A. B., and Giorgi, F.: Droughts and floods over the upper catchment of the Blue Nile and their connections to the timing of El Niño and La Niña events, Hydrol. Earth Syst. Sci., 18, 1239–1249, https://doi.org/10.5194/hess-18-1239-2014, 2014.

Zeleke, T., Giorgi, F., Mengistu Tsidu, G., and Diro, G. T.: Spatial and temporal variability of summer rainfall over Ethiopia from observations and a regional climate model experiment, Theor. Appl. Climatol., 111, 665–681, 2013.

Zeleke, T., Yeshita, B. D., and Agidew, F. M.: Evaluation of a Regional Climate Model for the Upper Blue Nile Region, in: Topics in Climate Modeling, edited by: Hromadka, T. and Rao, P., IntechOpen, Rijeka, https://doi.org/10.5772/64954, 2016.

Zeng, X., Zhao, M., and Dickinson, R. E.: Intercomparison of Bulk Aerodynamic Algorithms for the Computation of Sea Surface Fluxes Using TOGA COARE and TAO Data, J. Clim., 11, 2628–2644, 1998.